IEEE Photonics Journal
An IEEE Photonics Society Publication

Stability Studies on Continuous-Wave Broadband Generated in an Erbium-Doped Fiber Ring Laser Using Highly Nonlinear Fiber

Volume 2, Number 5, October 2010

Aditi Ghosh
Deepa Venkitesh
R. Vijaya, Senior Member, IEEE

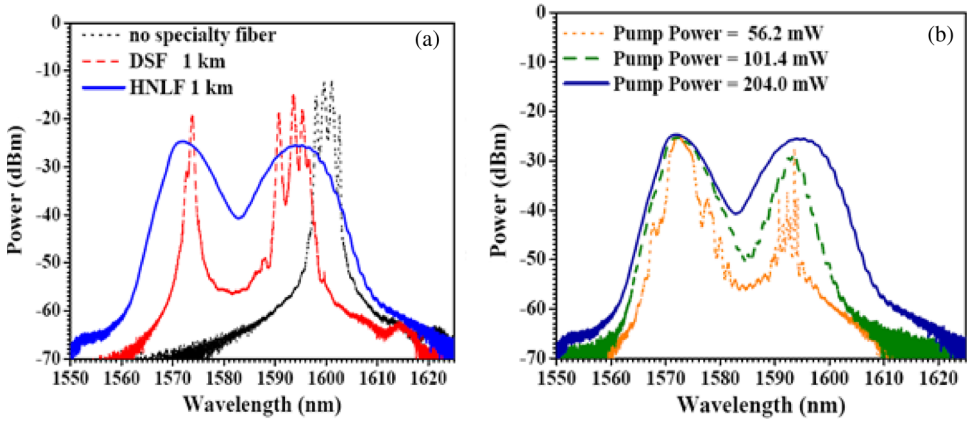

DOI: 10.1109/JPHOT.2010.2060318
1943-0655/$26.00 ©2010 IEEE

Stability Studies on Continuous-Wave Broadband Generated in an Erbium-Doped Fiber Ring Laser Using Highly Nonlinear Fiber

Aditi Ghosh,[1] Deepa Venkitesh,[2] and R. Vijaya,[1,3] *Senior Member, IEEE*

[1]Department of Physics, Indian Institute of Technology Bombay, Mumbai 400 076, India
[2]Department of Electrical Engineering, Indian Institute of Technology Madras, Chennai 600 036, India
[3]Department of Physics, Indian Institute of Technology Kanpur, Kanpur 208 016, India

DOI: 10.1109/JPHOT.2010.2060318

Manuscript received May 12, 2010; revised June 27, 2010; accepted July 11, 2010. Date of publication July 16, 2010; date of current version August 6, 2010. This work was supported by the Ministry of Information Technology, Government of India. Corresponding author: R. Vijaya (e-mail: rvijaya@iitk.ac.in).

Abstract: Continuous-wave (CW) broadband in the C- and L-band wavelength regions is demonstrated by introducing a highly nonlinear fiber (HNLF) in an erbium-doped fiber ring laser (EDFRL). A broadband spectrum of ~39 nm in the L-band and ~21 nm in the C-band were obtained at pump powers as low as ~200 mW with appropriate optimizations. Demultiplexed output from the broadband generated in the C-band region is tested for wavelength and power stability for consideration as a suitable source for various applications. The wavelength and power fluctuations have been observed to be at most ~0.02 nm and ~0.3 dBm, respectively.

Index Terms: Fiber laser, fiber nonlinear optics, laser stability.

1. Introduction

Optical broadband sources are expected to find cost-effective applications in wavelength-division multiplexing, sensing, optical component testing, biomedical imaging, and spectroscopy. A prominent medical application is in optical coherence tomography (OCT) [1], [2] since a broadband source can enable a high degree of axial resolution. Most sensor applications based on low-coherence interferometry require a broadband source with a high degree of spatial coherence, which is attainable in single-mode fiber-based laser designs. On the other hand, by using a suitable demultiplexer, a broadband source could be used as a multiwavelength source. Both multiwavelength as well as broadband emissions have been obtained using erbium-doped fiber lasers (EDFLs), primarily by utilizing different kinds of optical nonlinearities in a fiber such as stimulated Brillouin scattering (SBS) [3], Raman scattering [4]–[7], four-wave mixing (FWM) [8]–[10], and the use of specialty fibers [11]–[14]. However, the schemes of CW supercontinuum generation making use of nonlinear effects usually require high powers of the order of watts or require multiwavelength pumping. In an earlier work, it has been shown that EDFRL, without using an intracavity filter, is an ideal design to utilize the gain spectrum of the doped fiber for broadband generation, in conjunction with nonlinear effects in a dispersion shifted fiber (DSF) [12]. New frequencies generated due to the nonlinear effects in the fiber are amplified by the gain medium during multiple propagation of the intracavity field. The mechanism of spectral broadening can be understood from [12] and can be obtained by optimizing the cavity parameters for any specialty fiber.

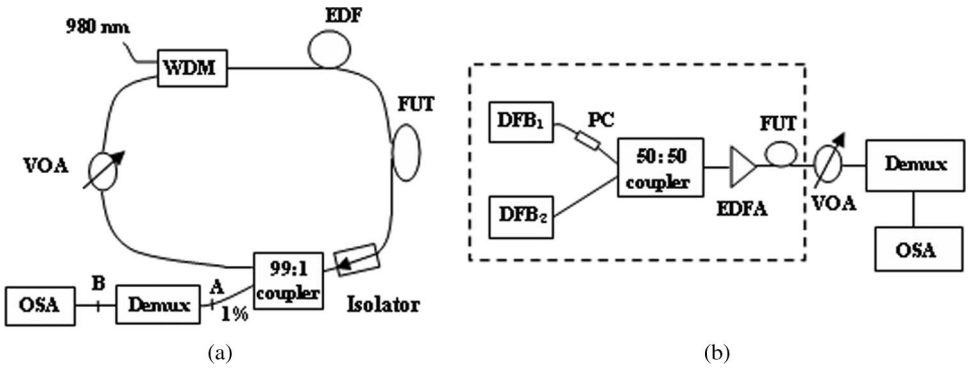

Fig. 1. Experimental setup for stability test on broadband generated in (a) ring cavity configuration including a nonlinear fiber and (b) mere propagation through a nonlinear fiber.

In the present work, broadband generation with a 20-dB spectral width $(\Delta\lambda)$ of $\sim$39 nm in the L-band and $\sim$21 nm in the C-band is demonstrated by introducing a highly nonlinear fiber (HNLF) in a filterless EDFRL using pump powers as low as $\sim$200 mW. The broadening is also studied for DSF under similar conditions for comparison, showing the higher efficiency of FWM in the case of HNLF in the cavity. The utility of the broadband source for communication systems is emphasized by studying the stability of the demultiplexed output in terms of wavelength drift, power drift, and average signal-to-noise ratio (SNR) for a significant duration of time. The test of the stability is essential in the case of broadband or multiwavelength sources as they could be limited by several sources of noise such as mode-partition noise, relative intensity noise [15], and optical beat noise [16]. The drift measurements have been compared with those from the nearly degenerate FWM of two wavelengths propagated through HNLF to highlight the advantages of the ring cavity configuration. The comparison is also carried out with the output of a fiber laser containing a DSF in the cavity, as well as that of a standard distributed feedback (DFB) laser source, which is an ideal source for high-bit-rate systems due to its innate wavelength and power stability [17]. The results clearly demonstrate the high stability of the broadband source generated by introduction of a HNLF in the filterless EDFRL.

2. Experimental Setup

The experimental setup as shown in Fig. 1(a) consists of a typical unidirectional ring cavity with a suitable length of EDF, pumped by a semiconductor laser diode operating at 980 nm. A wavelength-division multiplexer (WDM) is used to couple the pump power into the cavity. Ninety nine percent of the output power from the EDF is fed back into the input through a directional coupler, which completes the ring cavity structure. The remaining 1% tapped out of the cavity is monitored to study the spectral characteristics of the output. The resolution bandwidth of the optical spectrum analyzer (OSA) is 0.1 nm, and it can measure a minimum drift of 0.001 nm from a specified wavelength (reference) in drift-mode settings. An optical isolator is included in the cavity to avoid standing wave operation. The isolator also serves to block back-reflected power, if any, due to SBS. A variable optical attenuator (VOA) is introduced in the ring cavity for tunability of the spectrum [18]. Alternatively, if a spectral filtering element is used, the cavity gets locked at a chosen wavelength and limits the achievable spectral width. The types of fiber under test (FUT) used in the experiments are i) HNLF and ii) DSF. The broadband generated is observed on the OSA, which is connected at position A for this purpose. Due to the large length, the cavity supports multiple longitudinal modes.

The stability of the output is studied in the C-band by carrying out drift-mode measurements on a channel selected from the broadband using a demultiplexer (Demux). The Demux has an inter-channel spacing of 100 GHz with individual channel bandwidths (FWHM) lying between 0.17 nm to 0.18 nm. The insertion loss of the channels is $\sim$3.3 dB. The output of the Demux is fed into the OSA, which is now connected at position B. These drift-mode measurements evaluate variations in the spectral position, power, as well as the SNR with time.

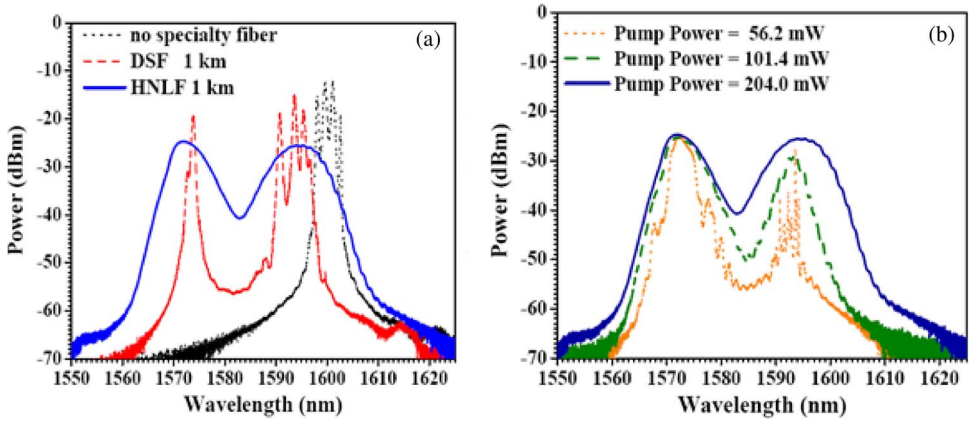

Fig. 2. (a) Spectral characteristics in the i) absence of any specialty fiber, ii) presence of DSF (1 km), and iii) presence of HNLF (1 km) in the EDFRL at a pump power of 204 mW. (b) Spectral characteristics of the output with HNLF (1 km) in the cavity and optimization with VOA at three different pump powers: 56.2, 101.4, and 204 mW.

For comparison, the stability test is also carried out in the case of i) FWM products obtained by mere propagation of closely spaced wavelengths through HNLF and ii) a DFB laser output. The experimental setup as shown in Fig. 1(b) for the former consists of two DFB lasers (DFB_1 and DFB_2) with center wavelengths of 1550.92 nm and 1550.12 nm, respectively. The outputs from these are polarization matched using a polarization controller (PC) for one of the channels and combined using a 50:50 coupler. The output of the coupler is amplified using an erbium-doped fiber amplifier (EDFA) and then propagated through HNLF (1 km) in which the efficient FWM process takes place, giving rise to sidebands at longer wavelengths (Stokes) and shorter wavelengths (anti-Stokes). The Demux selects the channels (the first-order Stokes and anti-Stokes) to be studied for drift measurements on the OSA. In the case of comparison with a standard DFB laser output, the dashed box [as shown in Fig. 1(b)] is replaced by a DFB laser tuned at the appropriate wavelength.

3. Results and Discussion

The center wavelength of lasing (λ_c) in a filterless laser is decided by the condition for which the loss in the cavity balances the gain. It is found from earlier experiments that the spectral width of the output of the filterless fiber laser increases slightly with an increase in pump power, even in the absence of a nonlinear element in the cavity due to gain saturation at the lasing wavelength resulting in a larger gain at the neighboring longitudinal modes [19], [20]. The spectral width can be enhanced substantially by introducing additional fibers in the cavity which have large nonlinear parameters and low dispersion. DSF/HNLF are introduced in the cavity, and the spectrum was observed at a maximum pump power of $\sim$200 mW. The DSF used in this work has a nonlinear parameter $\gamma = 2.4$ $W^{-1}km^{-1}$, zero-dispersion wavelength of 1544 nm, and a dispersion slope of 0.072 ps $km^{-1}nm^{-2}$. The experiments are repeated with HNLF (nonlinear parameter $\gamma = 12.4$ $W^{-1}km^{-1}$, zero-dispersion wavelength of 1513 nm, and a dispersion slope of 0.007 ps $km^{-1}nm^{-2}$). By a suitable choice of length and dopant concentration of the EDF in the cavity, the spectral broadening can be obtained in the C-band, the L-band, or both. These cases are discussed below.

3.1. L-Band Results

The experimental setup using EDF (Fibercore—model M12) of length 7 m in the cavity demonstrated lasing in the L-band. In this experimental configuration, for a pump power of 204 mW, the laser linewidth $\Delta\lambda$ in the absence of any additional fiber in the cavity is $\sim$5.7 nm, and λ_c is at 1600.6 nm [shown as dotted black line in Fig. 2(a)]. The addition of DSF (1 km) in the cavity increases the intracavity loss, resulting in a shift in λ_c to 1593 nm. A second peak is found to occur at 1573 nm along with the center wavelength, indicating that the low threshold conditions are

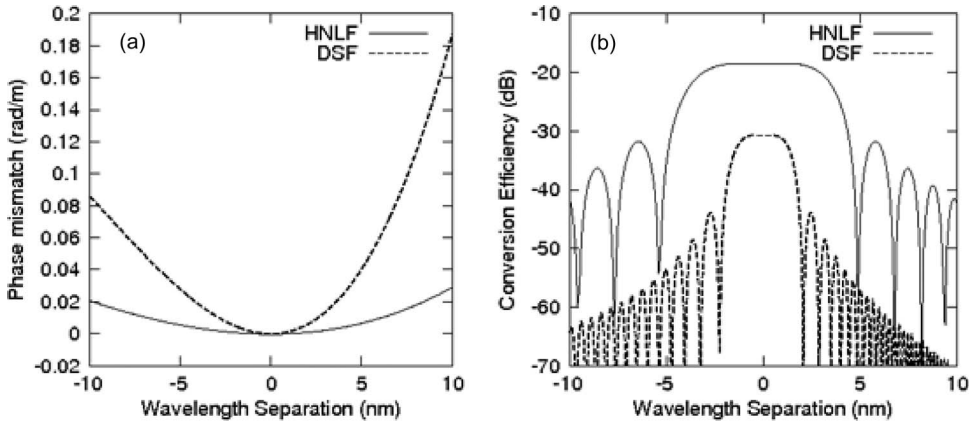

Fig. 3. Estimated variation of (a) phase mismatch and (b) conversion efficiency with wavelength separation for two adjacent longitudinal modes in DSF and HNLF for the first-order Stokes component.

satisfied for both these wavelength regions. An additional loss of 0.166 dB is introduced using VOA in the cavity such that the spectral width is optimized. Thus, introduction of DSF in the cavity results in two peaks centered at 1573 and 1593 nm, with bandwidths of 3 and 7.1 nm, respectively [shown as a dashed red line in Fig. 2(a)]. To enhance the nonlinear effects in the cavity, a HNLF (1 km) is now introduced (in place of DSF). With an additional loss of 1.2 dB introduced using the VOA, the wavelength of operation is shifted to a flat region in the gain spectrum, resulting in a larger spectral width of $\sim$39 nm in the L-band at a pump power of 204 mW (as shown in Fig. 2(a) with solid blue line), which clearly indicates the contribution due to the higher nonlinearity of the HNLF as compared with DSF.

An increase in pump power aids the nonlinear effects in the fiber, resulting in an increase in the spectral width. This is clear from Fig. 2(b), where the spectral characteristics of the output signal power are compared for HNLF (1 km) at pump powers of 56.2, 101.4 and 204 mW. The increase in spectral width with input pump power confirms the role of nonlinear effects in broadening. In addition, the smoothening of spectral features as more intermediate frequencies are generated at larger pump powers is also evident in Fig. 2(b). One may note that at lower pump power levels, the wavelengths around 1570 nm are saturated, and the spectral width around 1570 nm is larger than at 1600 nm, which is commensurate to that pump power. As the pump power increases, the FWM leads to additional wavelengths around both these wavelengths, which, in turn, seed further FWM.

In the case of ring cavity, the distribution of power in the FWM process and that lost due to linear attenuation is compensated by the gain due to EDF, and the new frequencies generated get amplified in each round trip by this gain. Introduction of HNLF has resulted in a smooth spectral feature, indicating a significant increase in the nonlinear mixing and the resulting spectral enrichment. The multiple longitudinal modes intrinsically supported by the cavity undergo several FWM processes, resulting in an increase in spectral broadening [20], [21]. The number of longitudinal modes is the same when equal lengths of HNLF and DSF are introduced, which implies that the better spectral enrichment with increased stability with HNLF is due to the difference in FWM efficiencies for the two fibers.

The FWM efficiency is decided by the phase matching conditions of the mixing frequencies. Phase mismatch is contributed through both dispersive and nonlinear phase. The method for estimation of phase mismatch and conversion efficiency for different wavelength separations in the case of DSF has been studied in detail in an earlier work [22]. To contemplate an improved efficiency and stability with the use of HNLF, consider the mixing of two adjacent longitudinal modes (with equal powers of 10 mW each) in the L band. The estimated variation of the total phase mismatch with the wavelength separation between the mixing longitudinal modes, in the case of Stokes sideband generation in DSF and HNLF, is shown in Fig. 3(a). One of the wavelengths was kept fixed at 1570 nm, whereas the other was varied $\pm$10 nm about this wavelength. Since the wavelength of operation lies in the anomalous dispersion region for both DSF and HNLF used in the

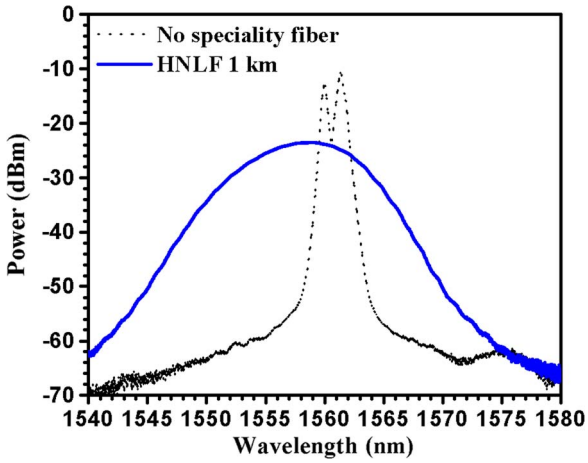

Fig. 4. Spectral characteristics in the C-band region in the presence and absence of HNLF in the EDFRL at a pump power of ~200 mW.

experiments, the contribution to the phase mismatch due to dispersion is negative, which can get compensated through the nonlinear phase (which is always positive). It can be observed from Fig. 3(a) that the resultant phase mismatch is close to zero for a larger wavelength range in the case of HNLF. This is attributed to i) smaller dispersion slope and hence a smaller dispersive phase and ii) better compensation through nonlinear phase due to the larger nonlinear parameter. Consequently, the estimated conversion efficiency for a given FWM product is found to be better than that of DSF, as seen in Fig. 3(b). The conversion efficiency is also found to remain constant for larger wavelength separation (up to 5 nm). Minima in conversion efficiency imply a loss in the cavity at that particular wavelength, which need to be compensated by the EDFA gain. After each round trip, if the loss corresponding to these minima is not completely compensated, it would result in instability at the output. The broadening observed experimentally is the result of many such mixing processes. Thus, smaller conversion efficiency and the occurrence of larger number of minima in the case of DSF are expected to drive the system to be unstable for larger wavelength separations.

3.2. C-Band Results

To obtain broadband in the C-band region, an EDF of lower dopant concentration (Fibercore—model M5) and length 3 m was used in the cavity. In this case, λ_c in the absence of any specialty fiber was at 1561.4 nm, with a $\Delta\lambda$ of 3.2 nm at a pump power of 210 mW (shown with dotted black line in Fig. 4). For the same reasons as stated earlier, introducing a HNLF (1 km) in the cavity results in spectral broadening. Optimizing the broadband hence obtained, by variation of the attenuation in the cavity (using a VOA), results in the spectrum as seen (with solid blue line) in Fig. 4. The optimum spectral width was obtained at an attenuation of 0.79 dB. As compared with the case of no specialty fiber, the center wavelength gets shifted to 1559.0 nm, and spectral width increases to 21.4 nm.

3.3. Stability Test and Comparison

The output of the laser can be characterized in numerous ways, including a test of its stability. A quantitative measurement is essential to evaluate its applications such as a multiwavelength source for DWDM applications. Demultiplexed output from the broadband generated is used for the test of the stability in terms of wavelength and power drift of the laser output. A measure of noise is also quantified by measuring the SNR at the output. These parameters are studied for 1 h, at a sampling rate of 1/min using an OSA. The measurements obtained for the fiber ring laser output with HNLF (1 km) in the cavity is compared with that obtained with a DSF of length 2.5 km in the cavity (this larger length was required for sufficient power at one of the demultiplexed output to be

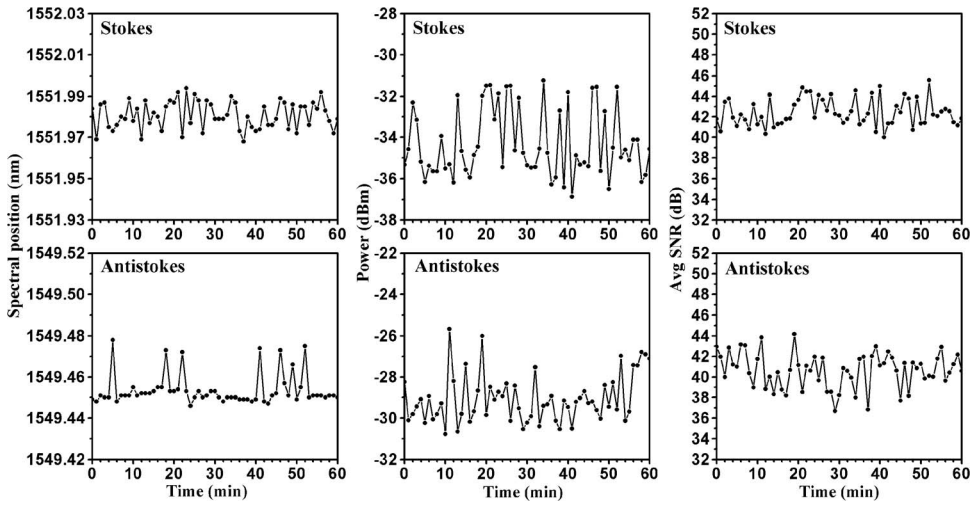

Fig. 5. Drift in the spectral position, power at the center wavelength, and average SNR with time after mere propagation through HNLF and demultiplexed for first-order Stokes and anti-Stokes side-bands.

tested). These results are also compared with that of a standard DFB laser output which has been, conventionally, the favorite choice as a source for communication. The linewidth of the demultiplexed source, however, depends on the filter used. Comparison with the FWM products obtained by mere propagation through HNLF emphasizes the superiority of the ring configuration. Multiple propagations in the cavity are expected to be better, as compared with mere propagation, in terms of efficiency of the nonlinear effects and stability of spectral position, as well as power.

The mere propagation output through HNLF is studied by analyzing the stability of the FWM products. The spectral position, power, and SNR, as obtained on the OSA, are shown in Fig. 5. The wavelength (spectral position) variation remained within the wavelength uncertainty limit of the OSA. There is a significant power and SNR variation observed in the drift results. The power fluctuations can be accounted for by SBS. The SNR variation is larger due to the larger variation in the power.

In the cavity configuration, significantly fewer drifts are expected as compared with the above results, because the introduction of a nonlinear fiber in the ring configuration results in a stable output [23]. The stability results are also compared with drift-mode measurements on a standard DFB laser output. The variation in spectral position and power fluctuations measured in the case of DFB laser are 0.008 nm and 0.47 dBm. After including DSF of length 2.5 km in the cavity, the output was demultiplexed, and the above parameters were measured. The wavelength and power fluctuations measured are 0.010 nm and 0.38 dBm, respectively. This is in agreement with the values obtained in the work by Chen *et al.* utilizing DSF in the cavity under similar experimental conditions [24]. The measurements were repeated with HNLF in the cavity for two demultiplexed outputs: Channel 16 (1555.90 nm) and Channel 15 (1555.06 nm) (which had sufficient power). The wavelength variation and power fluctuation measured for Channel 16 are 0.006 nm and 0.28 dBm and that for Channel 15 are 0.018 nm and 0.13 dBm (as shown in Fig. 6). The power variation is clearly less than that in the case of DSF. Comparing it with the stability of channel obtained by a multi-wavelength Brillouin-erbium fiber ring laser [25], the power fluctuations are of the order or better than the values obtained in their work. The wavelength variation in our case is more than that obtained in [25] (0.002 nm).

The values obtained from each stability test can be compared from Table 1. The average values for each parameter are represented in parentheses below the respective values. In the case of HNLF included in the cavity, the demuxed output (of a broadband) from both channels 15 and 16 are comparable with that of a DFB laser in stability of wavelength, power, and SNR. The power generated due to a nonlinear process is thus seen to be as stable as that obtained from a DFB laser. The wavelength drift is observed to be more for channel 15 as compared with channel 16,

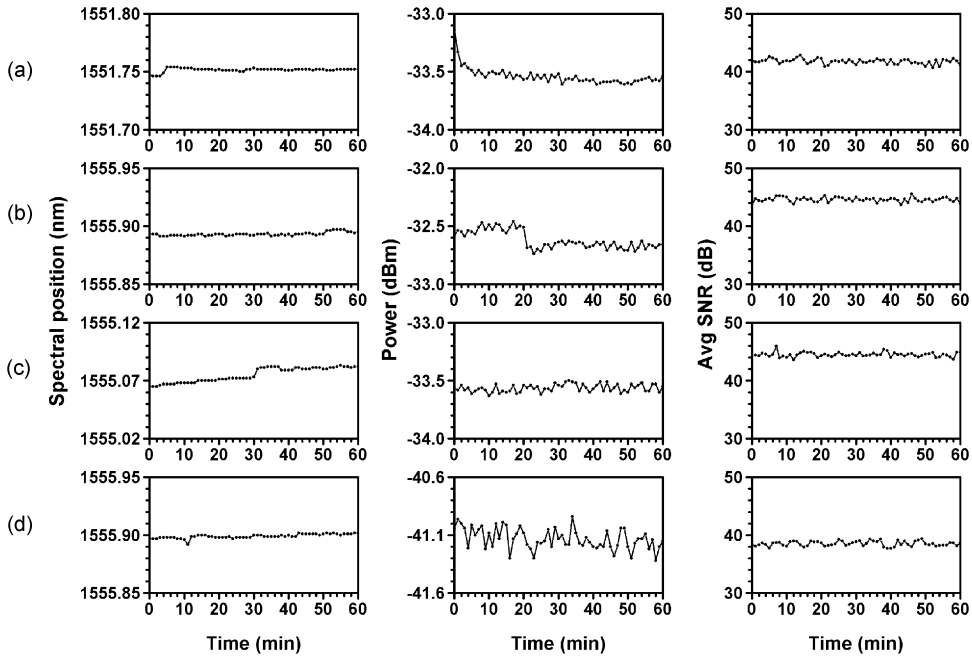

Fig. 6. Comparison of drift in the spectral position, power, and average signal to noise ratio with time of (a) DFB laser output: demux Channel 11, (b) fiber laser output (HNLF 1 km): demux Channel 16, (c) fiber laser output (HNLF 1 km): demux Channel 15, and (d) fiber laser output (DSF 2.5 km): demux Channel 16.

TABLE 1

Comparison of the variations in spectral position, power, and SNR from drift-mode measurements of FWM products after mere propagation, a standard DFB laser output, and demultiplexed output of a fiber ring laser including a nonlinear fiber (HNLF/DSF) in the cavity

Drift in	Mere propagation: HNLF 1 km (Stokes)	Mere propagation: HNLF 1 km (anti-Stokes)	DFB laser output	EDFRL with HNLF: 1km Channel 16	EDFRL with HNLF: 1km Channel 15	EDFRL with DSF: 2.5 km Channel 16
Spectral position (nm)	0.026 (1551.989)	0.032 (1549.449)	0.008 (1551.747)	0.006 (1555.893)	0.018 (1555.064)	0.010 (1555.898)
Power (dBm)	5.64 (-33.89)	5.11 (-28.34)	0.47 (-33.58)	0.28 (-32.48)	0.13 (-33.61)	0.38 (-41.30)
Average SNR (dB)	5.55 (41.07)	7.5 (41.79)	2.14 (41.87)	1.89 (45.37)	2.38 (44.34)	1.66 (38.78)

whereas the power drift is less for channel 15 as compared with 16. This is due to lesser efficiency of the FWM process for the wavelength corresponding to channel 15, but the power becomes stable due to multiple round trips in the cavity. In the case where DSF is studied, the SNR is lower, which is expected as the output power itself is lower in the case of DSF with its longer length of 2.5 km, but the power variation with time in the case of DSF showed a lot of fluctuations, as compared with all the above cases.

In comparison with the mere propagation results, it is clear from Table 1 that the output of the fiber laser ring cavity gives a much more stable output. Desired number of channels can be carved out

from the single broadband source. The cause of the power fluctuations such as Brillouin scattering in the former get countered in the unidirectional cavity configuration. The longitudinal mode mixing is a more coherent and stable process in the cavity. Hence, a stable broadband spectrum is obtained using an HNLF within the ring cavity configuration. The stability of the wavelength is an obvious necessity, especially in the case of optical communications, where the channel separation, as well as relative differences in the channel powers being within a certain limit, is mandatory. Apart from communications, the stable continuous-wave broadband sources are finding applications in the field of biomedical imaging, and the spectrum generated in our work is at considerably low pump powers. Thus, there is a scope of broader spectral width and, hence, improved axial resolution with access to higher powers. However, this work focuses on the study of generation of highly stable broadband at low pump powers available in a compact configuration and has wide applicability.

4. Conclusion

By introducing a 1-km length of HNLF in the cavity of a filterless EDFRL, a broadband of spectral width $\sim$39 nm in the L-band and $\sim$21 nm in the C-band is demonstrated at pump powers of $\sim$200 mW. The higher nonlinear coefficient of the HNLF leads to a broader spectrum in comparison with DSF. Drift measurements of spectral position, power and average SNR on the demultiplexed output from the broadband show that, in terms of stability, this system is comparable with a standard DFB laser, which is an ideal choice for numerous applications. Moreover, a stable multiwavelength source is cost-effective. The applicability of the present source for WDM systems could be further ratified with propagation experiments using PRBS data modulated on these demultiplexed wavelengths at higher pump powers. The superiority of the efficiency of FWM and stability in a ring configuration over the mere propagation configuration is also evident from the above analysis, thus making a ring laser configuration a better choice for the generation of broadband/ multiwavelength emission.

References

[1] D. Huang, E. Swanson, C. P. Lin, J. S. Schuman, W. G. Stinson, W. Chang, M. R. Hee, T. Flotte, K. Gregory, C. A. Puliafito, and J. G. Fujimoto, "Optical coherence tomography," *Science*, vol. 254, no. 5035, pp. 1178–1181, Nov. 1991.

[2] J. G. Fujimoto, M. E. Brezinski, G. J. Tearney, S. A. Boppart, B. E. Bouma, M. R. Hee, J. F. Southern, and E. A. Swanson, "Optical biopsy and imaging using optical coherence tomography," *Nature Med.*, vol. 1, no. 9, pp. 970–972, Sep. 1995.

[3] M. P. Fok and C. Shu, "Spacing-adjustable multi-wavelength source from a stimulated Brillouin scattering assisted erbium-doped fiber laser," *Opt. Express*, vol. 14, no. 7, pp. 2618–2624, Apr. 2006.

[4] M. G. Herraez, S. Martin-Lopez, P. Corredera, M. L. Hernanz, and P. R. Horsche, "Supercontinuum generation using a continuous wave Raman fiber laser," *Opt. Commun.*, vol. 226, no. 1–6, pp. 323–328, Oct. 2003.

[5] W. Zhang, Y. Wang, J. Peng, and X. Liu, "Broadband high power continuous wave fiber Raman source and its applications," *Opt. Commun.*, vol. 231, no. 1–6, pp. 371–374, Feb. 2004.

[6] A. A. Babin, D. V. Churkin, A. E. Ismagulov, S. I. Kablukov, and E. V. Podivilov, "Spectral broadening in Raman fiber lasers," *Opt. Lett.*, vol. 31, no. 20, pp. 3007–3009, Oct. 2006.

[7] M. Prabhu, A. Taniguchi, S. Hirose, J. Lu, M. Musha, A. Shirakawa, and K. Ueda, "Supercontinuum generation using Raman fiber laser," *Appl. Phys. B, Photophys. Laser Chem.*, vol. 77, no. 2/3, pp. 205–210, Sep. 2003.

[8] X. Liu, X. Zhou, and C. Lu, "Four-wave mixing assisted stability enhancement: Theory, experiment and application," *Opt. Lett.*, vol. 30, no. 17, pp. 2257–2259, Sep. 2005.

[9] Y. G. Han and S. B. Lee, "Flexible tunable multi-wavelength erbium doped fiber laser based on four-wave mixing effect in dispersion-shifted fibers," *Opt. Express*, vol. 13, no. 25, pp. 10 134–10 139, Dec. 2005.

[10] Y. G. Han, T. V. A. Tran, and S. B. Lee, "Wavelength spacing tunable multiwavelength erbium-doped fiber laser based on four-wave mixing of dispersion-shifted fiber," *Opt. Lett.*, vol. 31, no. 6, pp. 697–699, Mar. 2006.

[11] X. Liu, X. Xhou, X. Tang, J. Ng, J. Hao, T. Y. Chai, E. Leong, and C. Lu, "Switchable and tunable multiwavelength erbium-doped fiber laser with fiber Bragg gratings and photonic crystal fiber," *IEEE Photon. Technol. Lett.*, vol. 17, no. 8, pp. 1626–1628, Aug. 2005.

[12] D. Venkitesh and R. Vijaya, "Spectral characteristics of continuous wave broadband from a fiber laser with a low dispersion fiber in the cavity," *J. Appl. Phys.*, vol. 104, no. 5, pp. 053104-1–053104-5, Sep. 2008.

[13] S. Pan, C. Lou, and Y. Gao, "Multiwavelength erbium-doped fiber laser based on inhomogeneous loss mechanism by use of a highly nonlinear fiber and a Fabry–Perot filter," *Opt. Express*, vol. 14, no. 3, pp. 1113–1118, Feb. 2006.

[14] J. H. Lee, Y. Takushima, and K. Kikuchi, "Continuous-wave supercontinuum laser based on an erbium-doped fiber ring cavity incorporating a highly nonlinear optical fiber," *Opt. Lett.*, vol. 30, no. 19, pp. 2599–2601, Oct. 2005.

[15] J. Poette, S. Blin, G. Brochu, L. Bramerie, R. Slavik, J.-C. Simon, S. LaRochelle, and P. Besnard, "Relative intensity noise of multiwavelength fibre laser," *Electron. Lett.*, vol. 40, no. 12, pp. 724–725, Jun. 2004.

[16] A. Banerjee, Y. Park, F. Clarke, H. Song, S. Yang, G. Kramer, K. Kim, and B. Mukherjee, "Wavelength-division-multiplexed passive optical network (WDM-PON) technologies for broadband access: A review," *J. Opt. Netw.*, vol. 4, no. 11, pp. 737–758, Nov. 2005.
[17] M. Ibsen, S. Alam, M. Zervas, A. B. Grudinin, and D. N. Payne, "8- and 16-channel all-fiber DFB laser WDM transmitters with integrated pump redundancy," *IEEE Photon. Technol. Lett.*, vol. 11, no. 9, pp. 1114–1116, Sep. 1999.
[18] V. Deepa and R. Vijaya, "Effect of pump power on the tuning range of a filterless erbium-doped fiber ring laser," *Appl. Phys. B, Photophys. Laser Chem.*, vol. 89, no. 2/3, pp. 329–332, Nov. 2007.
[19] V. Deepa and R. Vijaya, "Linewidth characteristics of a filterless tunable erbium doped fiber ring laser," *J. Appl. Phys.*, vol. 102, no. 8, pp. 083107-1–083107-6, Oct. 2007.
[20] V. Roy, M. Piche, F. Babin, and G. W. Schinn, "Nonlinear wave mixing in a multi longitudinal mode erbium doped fiber laser," *Opt. Express*, vol. 13, no. 18, pp. 6791–6797, Sep. 2005.
[21] J. C. Bouteiller, "Spectral modeling of Raman fiber lasers," *IEEE Photon. Technol. Lett.*, vol. 15, no. 12, pp. 1698–1700, Dec. 2003.
[22] R. Deepa and R. Vijaya, "Generalised dispersive phase and its effect on four wave mixing in fibers," *Opt. Commun.*, vol. 269, no. 1, pp. 206–214, Jan. 2007.
[23] X. Liu, X. Yang, F. Lu, J. Ng, X. Zhou, and C. Lu, "Stable and uniform dual-wavelength erbium-doped fiber laser based on fiber Bragg gratings and photonic crystal fiber," *Opt. Express*, vol. 13, no. 1, pp. 142–147, Jan. 2005.
[24] D. Chen, S. Qin, Y. Gao, and S. Gao, "Wavelength-spacing continuously tunable multiwavelength erbium-doped fibre laser based on DSF and MZI," *Electron. Lett.*, vol. 43, no. 9, pp. 524–525, Apr. 2007.
[25] M. Ajiya, M. A. Mahdi, M. H. Al-Mansoori, S. Hitam, and M. Mokhtar, "Seamless tuning range based-on available gain bandwidth in multiwavelength Brillouin fiber laser," *Opt. Express*, vol. 17, no. 8, pp. 5944–5952, Apr. 2009.